More than just CO_2-recycling: corticular photosynthesis as a mechanism to reduce the risk of an energy crisis induced by low oxygen

Christiane Wittmann and Hardy Pfanz

Department of Applied Botany and Volcano Biology, University of Duisburg-Essen, Essen 45117, Germany

Author for correspondence:
Christiane Wittmann
Tel: +49 2011833122
Email: christiane.wittmann@uni-due.de

Received: *20 November 2017*
Accepted: *19 March 2018*

New Phytologist (2018)
doi: 10.1111/nph.15198

Key words: bark photosynthesis, CO_2 fluxes, corticular photosynthesis, hypoxia, stem CO_2-recycling, superoxia, xylem sap.

Summary

- Reassimilation of internal CO_2 via corticular photosynthesis (PS_{cort}) has an important effect on the carbon economy of trees. However, little is known about its role as a source of O_2 supply to the stem parenchyma and its implications in consumption and movement of O_2 within trees.
- PS_{cort} of young *Populus nigra* (black poplar) trees was investigated by combining optical micro-optode measurements with monitoring of stem chlorophyll fluorescence.
- During times of zero sap flow in spring, stem oxygen concentrations (cO_2) exhibited large temporal changes. In the sapwood, over 80% of diurnal changes in cO_2 could be explained by respiration rates ($R_{d(mod)}$). In the cortex, photosynthetic oxygen release during the day altered this relationship. With daytime illumination, oxygen levels in the cortex steadily increased from subambient and even exhibited a diel period of superoxia of up to 110% (% air sat.). By contrast, in the sapwood, cO_2 never reached ambient levels; the diurnal oxygen deficit was up to 25% of air saturation.
- Our results confirm that PS_{cort} is not only a CO_2-recycling mechanism, it is also a mechanism to actively raise the cortical O_2 concentration and counteract temporal/spatial hypoxia inside plant stems.

Introduction

The benefits of stem CO_2-recycling have been expressed in several recent comments and letters (Trumbore *et al.*, 2013; Cernusak & Cheesman, 2015; Vandegehuchte *et al.*, 2015). The term corticular photosynthesis (Wittmann *et al.*, 2006; Berveiller *et al.*, 2007) or stem recycling photosynthesis (Ávila *et al.*, 2014) stands for a syndrome in which chlorophyllous cells in the cortex of shrub and tree species refix a portion of the CO_2 respired by the underlying tissues or carried into the stem segment by the transpiration stream (Pfanz *et al.*, 2002; Teskey *et al.*, 2008; Ávila *et al.*, 2014; Cernusak & Cheesman, 2015). Tracer studies by Powers & Marshall (2011) as well as Bloemen *et al.* (2013) in temperate tree species showed that ^{13}C-labelled CO_2 added to the xylem stream is transported upward, and emitted to the atmosphere. A certain fraction is refixed in photosynthetic tissues in branches and petioles. Hence, recycling of CO_2 within trees is potentially important for the carbon economy of trees.

Oxygen is an indispensable substrate for many biochemical reactions (van Dongen & Licausi, 2015) in plants. Nevertheless, unlike animals, plants lack an active transport mechanism to distribute oxygen to all cells. In photosynthesis, oxygen is produced from the photolysis of water by photosystem II in the thylakoid membranes, thereby converting light energy into chemical energy in the forms of ATP and $NADPH_2$ (van Dongen & Licausi, 2015). Thus, besides recycling of internal carbon, corticular photosynthesis (PS_{cort}) is a source of molecular oxygen within woody stems. Aerobic metabolism by definition requires the presence of oxygen, which serves as the terminal electron acceptor for oxidative phosphorylation, a fundamental component of respiration. The effects of low oxygen on respiration are relatively clear: respiration decreases with decreasing O_2 concentration (Spicer & Holbrook, 2005). Inhibition of respiration is seen at roughly 0.01–0.1% O_2 in leaf mitochondria (Millar *et al.*, 1994), 0.5–2.5% in leaf protoplasts (Lammertyn *et al.*, 2001), 10% in roots (Saglio *et al.*, 1994) and 10–20% in tuber slices (Geigenberger *et al.*, 2000), but almost no data are available for woody stems.

All studies on stem recycling photosynthesis made thus far were focused on carbon fluxes and the process of carbon recycling within the cortex of stems. Oxygen fluxes in tree stems and the contribution of PS_{cort} to the oxygen status of stems has been almost never accounted for in experiments on stem photosynthesis (Wittmann & Pfanz, 2015). Figure 1 (right) shows the important gas fluxes in a stem segment of a tree. Part of the carbon released as CO_2 by respiring cells in the tree stem diffuses directly into the atmosphere (Fig. 1, step 1a–c), whereas another portion of this respired CO_2 remains inside the stem where it can diffuse in the radial (Fig. 1, step 2a–c) or in the axial direction (Fig. 1,

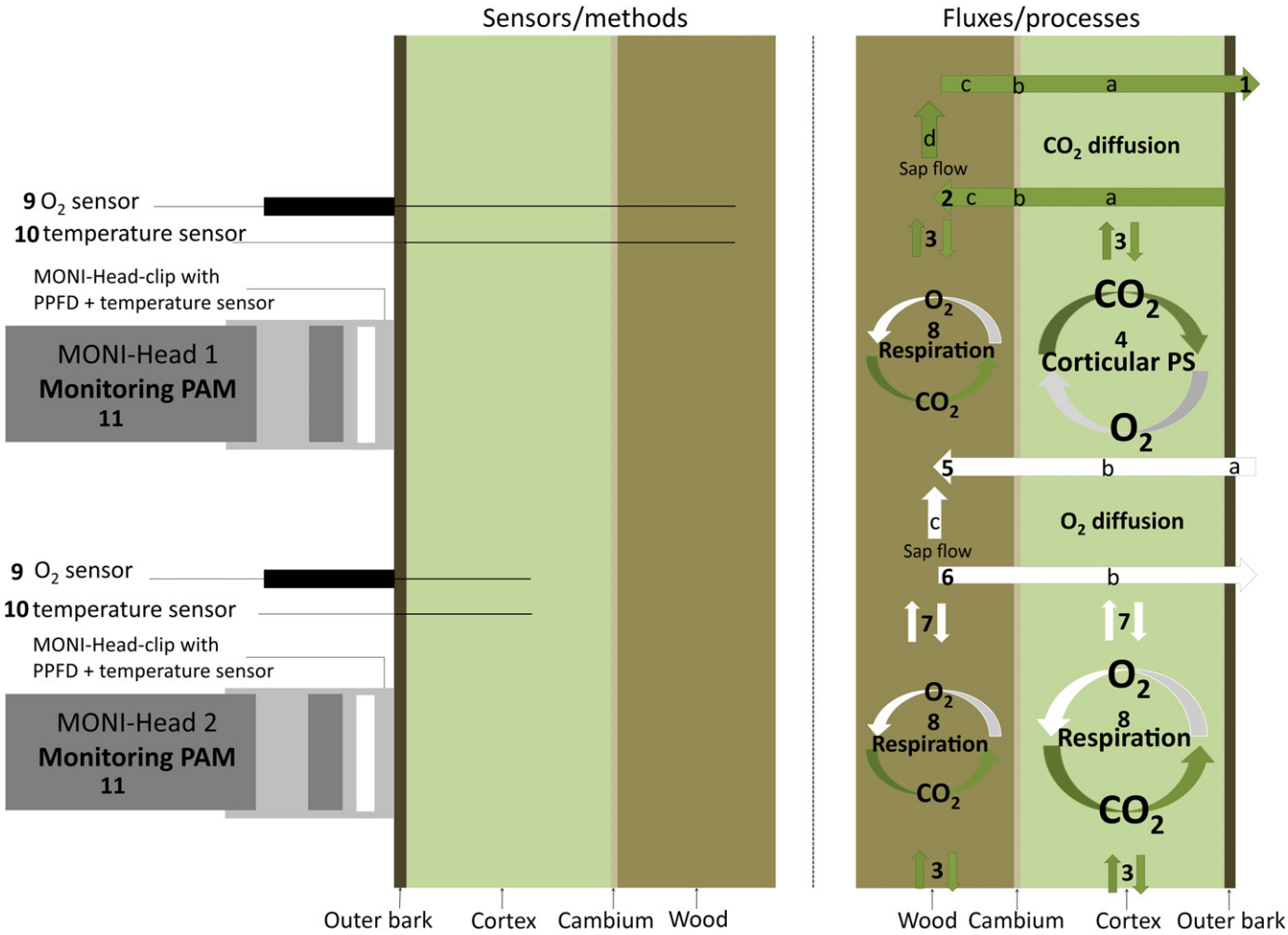

Fig. 1 Schematic of methods and sensors used (left) and of important processes and fluxes inside a stem segment of a tree (right): (1) radial diffusion of CO_2 out of the stem from cortex (a), cambium (b) and wood parenchyma cells (c), or imported in xylem sap (d); (2) radial diffusion of CO_2 into the stem from cortex (a), cambium (b) and wood parenchyma cells (c); (3) axial CO_2 diffusion in the cortex and wood; (4) CO_2 fixation by corticular photosynthesis, which can utilize CO_2 from all four sources and evolves oxygen as a byproduct (a–d). (5) radial diffusion of O_2 into the stem from atmosphere (a), cortex (b), or imported in xylem sap (c); (6) radial diffusion of O_2 out of the stem from cortex (b), or imported in xylem sap (c); (7) axial O_2 diffusion in the cortex and wood; (8) O_2 consumption by respiration, which can ultilize O_2 from all three sources (a, b, c). (9) Utilization of optical, oxygen microsensors for *in situ* measurement of tissue oxygen levels. (10) For temperature compensation of the oxygen measurements temperature sensors (Micro-T-type thermocouples with a tip-diameter of 0.7 mm) were inserted into the cortex and wood tissue of the main stems. (11) Continuous chlorophyll fluorescence measurments with a 'Monitoring-PAM Multi-Channel Chlorophyll Fluorometer' or MONI-PAM (Walz). Two robust and weather-resistent measuring heads (MONI-head/485), recording PAM fluorescence, temperature and PPFD, were installed on the main stem of each tree with a MONI-head-clip. It has to be considered that, according to the higher solubility of CO_2 in water, the transpiration stream functions as a vastly greater aqueous pathway for CO_2 transport than for O_2 transport. The schematic is not true to scale. Adapted from Steppe *et al.* (2015), with permission from Elsevier.

step 3), dissolve in xylem sap and be transported away from the site of origin (Fig. 1, step 1d). CO_2 fixation by PScort can utilize CO_2 from all four sources (Fig. 1, step 4) and reduces the amount of CO_2 escaping into the atmosphere on average by 72% (Cernusak & Marshall, 2000; Wittmann *et al.*, 2001; Pfanz *et al.*, 2002; Teskey *et al.*, 2008; Ávila *et al.*, 2014). However, oxygen could diffuse directly from the atmosphere into the stem (Fig. 1, step 5), because the gaseous environment within the woody stems is enriched in CO_2 and depleted in O_2 (Mugnai & Mancuso, 2010). Furthermore, oxygen released by PScort (Fig. 1, step 4) could remain in the stem where it can diffuse in the radial (outward or inward) or in the axial direction (upward or downward), dissolve in xylem sap and be transported away from the site of origin (Fig. 1, steps 5–7) or consumed by local respiration (Fig. 1, step 8). Studies of del Hierro *et al.* (2002) and Mancuso & Marras (2003) showed that the oxygen concentration of xylem sap ranges from a minimum in the absence of transpiration to a maximum during times of peak flow, suggesting that the transpiration stream is an important source of O_2. Other authors support the idea of a dual oxygen transport system within stems that supplies the stem parenchyma with oxygen via radial gas diffusion, via axial flow of oxygen dissolved in the xylem sap or via both (Hook *et al.*, 1972; Eklund, 2000; Gansert *et al.*, 2001; Spicer & Holbrook, 2005). We hypothesize that PScort acts as a

further important source of O_2 which might allow the cells of stems to survive phases of daily oxygen shortage. Especially during times of zero sap flow before bud burst, the oxygen evolved by PScort might be of increased importance in avoiding or reducing stem internal hypoxia. The phloem, as part of the cortex, represents a specialized transport tissue with high metabolic activity and high respiration rates (van Bel & Knoblauch, 2000) to provide ATP for active import and transport of sucrose (Stadler *et al.*, 1995), and this will result in high local rates of oxygen consumption. Thereby, it has to be considered that respiration or O_2 consumption also can be affected by diurnal changes in carbohydrate availability (e.g. phloem activity). Rates of stem and root respiration have already been linked to the availability of current photosynthate (Johnsen *et al.*, 2007).

Our hypothesis was tested on tree saplings of black poplar grown outside in the botanical garden of the University of Duisburg-Essen. By continuous *in situ* measurements of cortex and sapwood O_2 levels using needle-type oxygen microsensors and of stem chlorophyll fluorescence using a 'Monitoring-PAM chlorophyll fluorometer' and relating them to environmental conditions over the course of the day, the influence of irradiance and temperature on PScort and stem respiration were assessed.

As tree stems are far from being homogeneous, major physiological processes such as photosynthesis (oxygen source) and respiration (oxygen sink) do not occur in an uniform manner within and across stem tissues. When oxygen supply does not correspond to the demand, steep gradients of oxygen could occur inside stem tissues, which might provide a strong diffusion potential to drive a flux of oxygen from sites of high to those of low concentration. We addressed this by laboratory experiments performed on detached stem segments of black poplar trees. Chlorophyll fluorescence imaging techniques were used as an indirect measure of the spatial pattern of oxygen evolution (photosynthesis) among the stem cross-sections of black poplar. In addition, oxygen gas exchange measurements were performed directly on isolated cortex and wood tissues to determine the oxygen consumption rates of each tissue fraction in dependence on temperature and tissue oxygen. The results of gas exchange measurements also were used to model diurnal changes in tissue dark respiration rates ($R_{d(mod)}$) and to link changes in tissue O_2 levels to the underlying physiological processes (photosynthesis/respiration).

We hope the design of our experiments can help to investigate the diurnal characteristics of PScort, and hence to elucidate the regulation mechanisms and the physiological significance of PScort, and to bring this process into the spotlight not only as a mechanism of internal CO_2 recycling, but also as a weapon against low oxygen stress in tree stems.

Materials and Methods

Study site and experimental set-up

The study was conducted in March 2014 (before bud burst) on black poplar trees (*Populus nigra* L.) grown outside in the botanical garden of the University Duisburg-Essen (Germany). Trees were grown outside in 50-l plastic containers under sufficient nutrition (Einheitserde Typ T, Balster, Germany) and water supply, realized by periodic fertilization with Osmocote (Bayer, Leverkusen, Germany) and daily irrigation. Stems averaged 2.3 cm in diameter at soil level, and were on average 2.5 m in height. Experiments were divided in two parallel strands: laboratory experiments and *in situ* measurements under field conditions. For laboratory experiments, 4-yr-old main stems with a mean diameter of 10.15 ± 0.74 mm (Table 1) of ten different trees were sampled at breast height. *In situ* measurements were performed on three other trees. The general experimental set-up for the *in situ* measurements is shown in Fig. 1 (left). We focused on a comparatively small number of trees, because we had limited equipment for detailed continuous measurements. Measurements were made from 7 March–14 March 2014 on trees 1 and 2. From 14 March–20 March 2014 the same sensors were used for continuous measurements on Tree 3.

Laboratory experiments

Chlorophyll extraction For chlorophyll extraction, a 1-cm-long segment of each sampled stem ($n = 10$) was separated into cortex and wood fractions. Each fraction was cut in small pieces and placed in 80% (v/v) dimethyl sulfoxide (DMSO). Pigment extraction required *c.* 2 h at 65°C in the dark. To avoid acidification and a concomitant phaeophytinization of the chlorophylls, 20 mg $Mg_2(OH)_2CO_3$ was added. Finally, extract absorbances were measured with a spetromphotometer (UV 160; Shimadzu, Tokyo, Japan) and pigment contents calculated according to standard equations (Wellburn, 1994).

Peridermal PPFD transmission In order to determine Photosynthetic Photon Flux Density (PPFD), outer bark layers of stems were first carefully removed with a cork borer. Then, transmittance spectra between 380 and 720 nm were obtained by a high-resolution fiber optic spectrometer (HR4000; Ocean

Table 1 Morphometric parameters, chlorophyll contents and ratios of 4-yr-old stems of *Populus nigra* trees

Tissue/organ	Parameter	
Stem	Stem diameter (mm)	10.15 ± 0.74
Cortex	Tissue thickness (mm)	0.71 ± 0.09
Wood	Tissue thickness (mm)	3.82 ± 0.55
Cortex	Chl*a* (mg g^{-1} FW)	0.290 ± 0.040
	Chl*b* (mg g^{-1} FW)	0.150 ± 0.020
	Chl(*a*+*b*) (mg g^{-1} FW)	0.440 ± 0.060
	Chl(*a*+*b*) (mg m^{-2})	391.7 ± 30.1
	Chl*a*/*b*	1.91 ± 0.22
Wood	Chl*a* (mg g^{-1} FW)	0.010 ± 0.002***
	Chl*b* (mg g^{-1} FW)	0.015 ± 0.003***
	Chl(*a*+*b*) (mg g^{-1} FW)	0.025 ± 0.004***
	Chl*a*/*b*	0.64 ± 0.06***

Mean ± 1 SD of 10 independent measurements ($n = 10$).
Significant differences between pigment content or pigment ratio of cortex and wood as examined by Student's *t*-tests: *, $P < 0.05$; **, $P < 0.01$; ***, $P < 0.001$.

Optics, Ostfildern, Germany) equipped with a fiberoptic probe (fiber type: VIS/NIR, QP400-2-VIS/BX; Ocean Optics). A 100 W quartz halogen lamp (Xenophot HLX 64625; Osram, München, Germany) served as the radiation source. To avoid warming of the samples the radiation source was additionally equipped with an infrared filter (NIR filter ST 931619/KB, Balzers, Liechtenstein). For more details see Wittmann & Pfanz (2015). Samples were taken from 4-yr-old main stems of ten different trees ($n = 10$).

Chlorophyll fluorescence pattern of stem surfaces and among stem cross-sections Before sample preparation and measurements, stems were dark-adapted for 2 h. Images of fluorescence parameters (F_v/F_m, $\Delta F/F'_m$) of stem surfaces and among stem cross-sections of *P. nigra* were made with the standard version of IMAGING-PAM (Walz, Effeltrich, Germany). First, chlorophyll fluorescence parameters of 4-yr-old main stems of ten different trees were recorded. Then stems were dissected in 0.4-cm-thick pieces (Microtom Leica RM2025, Wetzlar, Germany) and cross-sections were placed on the centre of the platform base of the mounting stand (IMAG-S) of the IPAM. Sample preparation was performed at a room light of 4–5 photosynthetically active radiation (PAR) (μmol photons m^2 s^{-1}), but before the start of measurements samples were kept in total darkness for another 20 min. Preliminary trials indicated that the risk of dehydration of stem cross-sections during measurements could be neglected if they were put on top of moistened filter papers within petri dishes. In this case, photosystem II (PSII) efficiency of the stem tissues was stable for at least 1 h.

First images of F_v/F_m were determined. Afterwards the effective quantum yield ($\Delta F/F'_m$) of PSII was measured under an actinic light intensity of 15, 25, 45 and 80 μmol photons m^{-2} s^{-1} using the light-curve program of IPAM. The time interval during actinic illumination was set to 120 s. Room temperatures during the experiment were held constant (20 ± 0.5°C) by means of an air conditioning unit (GEA, Düsseldorf, Germany).

Additionally, images of PAR-absorptivity (abs) of stem surfaces and stem cross-sections were determined. The abs parameter as determined by the Standard Imaging-PAM can be considered as a close estimate of PAR-absorptivity. The apparent absorptivity is calculated pixel by pixel from the red (R)- and near-infrared (NIR)-images using the formula:

$$\text{Abs} = 1 - \text{R/NIR}. \qquad \text{Eqn 1}$$

Oxygen gas-exchange measurements of isolated stem tissues Oxygen consumption of stem tissues was measured using two Hansatech DW2/2 liquid-phase oxygen electrode systems with DW2 electrode chambers (Hansatech, King's Lynn, UK). All measurements were done on dark-adapted (at least 2 h) stems. Therefore, 4-yr-old main stems from ten different black poplar trees were sampled *ante meridiem* directly before the measurements. Before sampling, stems were covered with aluminium foil to prevent illumination of any kind. In the laboratory, the aluminium foil was removed and from each stem a 1-cm-long segment was cut and immediately transferred into incubation medium. Diffusion barriers within stems would affect gas diffusion rates. To minimize this potential source of error we worked with isolated stem tissues of small size. We used the cortex, after removal of the outer bark, and a thin layer of the outer wood fraction for gas exchange measurements. After tissue preparation, isolated tissues were again transferred into incubation medium and shaded until start of the measurements. All measurements were made at a thermostatically controlled (LAUDA ECO RE 415 S, Lauda-Königshofen, Germany) temperature within an oxygen-saturated (*c.* 250 μmol l^{-1} at 20°C) incubation medium (for details see Wittmann & Pfanz, 2015), buffered at pH 6. By stirring, restricted diffusion through the aqueous medium and boundary layers were further eliminated. Calibrations and calculations were described by Walker (1987). All measurements of temperature response of dark respiration (R_d) were made as follows: (i) samples were left to dark-adapt for at least 15 min at a temperature of 5°C until a steady rate of R_d was attained. (ii) temperature was increased by 5°C and samples were left to adapt to the chosen temperature for further 15 min until a steady-state rate of O_2 evolution was recorded; and (iii) the samples were exposed to the next temperature step. Measurements were made in the same manner at 10, 15 and 20°C.

In order to determine the optimal oxygen concentration for R_d of cortex and wood tissues of poplar stems we monitored the oxygen consumption at 20°C vs the oxygen concentration in the incubation medium bathing the respective stem tissue. Oxygen concentration within the incubation medium was saturated with oxygen by bubbling with air. Afterwards, decreasing oxygen concentrations were achieved by stepwise bubbling of the medium with oxygen-free N_2 gas. For measurements of gas exchange rates, samples were left to adapt to the respective oxygen concentration for at least 15 min until a steady rate of R_d was attained. To ensure total gas tightness of the electrode during measurements and to prevent any diffusion of oxygen from the atmosphere into the incubation medium the plunger cap and nut were additionally sealed with a sealant (Terostat; Henkel, Düsseldorf, Germany).

Before use, all samples were carefully infiltrated with incubation medium. Therefore, they were placed in a 50-ml plastic syringe with 20 ml incubation medium (assay buffer) and all air was removed. A gentle vacuum was created by withdrawing the plunger. During the vacuum the syringe was agitated to dislodge any gas bubbles from the surface of the tissues. The vacuum was released and a slight positive pressure was applied.

Working with excised tissues could alter O_2 gas exchange by inducing wound respiration. To determine whether excision influenced our measurements, we left samples from all isolated stem tissues 90 min in the dark recording the O_2 gas exchange. Oxygen consumption increased transiently to reach a steady-state rate within 15 min. In the following 70 min no changes in oxygen exchange rate were found, indicating that excision had not greatly altered O_2 gas exchange. Furthermore, it must be considered, that after excision, nonstructural carbohydrate supply to the sampled tissue is impeded and could potentially limit respiration rates and metabolic activity (Cannell & Thornley, 2000).

Field experiments ***Modelling of tissue respiration rates.*** The natural logarithm of the dark respiration rate (R_d), obtained by gas exchange measurements (see earlier), and the cortex or sapwood tissue temperature (T) were regressed using a linear model:

$$\log_e(R_d) = \beta_0 + \beta_1 T, \qquad \text{Eqn 2}$$

where β_0 and β_1 are the regression coefficients.

Q_{10} was calculated (Linder & Troeng, 1981) from:

$$Q_{10} = \exp(10\beta_1), \qquad \text{Eqn 3}$$

where β_1 is the regression coefficient obtained from Eqn 2.

For estimation of tissue respiration rate $R_{d(mod)}$ at a given temperature T, we substituted the measured value of T into Eqn 2 and took the exponential.

Oxygen measurement with optical microsensors. For oxygen measurements an OXY-4 micro-system with needle-type oxygen microsensors was used (PreSens GmbH, Regensburg, Germany). The needle-type oxygen microsensor consists of a plastic syringe (diameter = 7 mm), which houses the optical fibre. The oxygen sensitive flat-broken tip of the fibre (diameter < 140 µm) is protected inside a stainless steel needle (cannula diameter = 0.4 mm, length = 40 mm) and can be extended after tissue penetration with the help of a plunger. Optical microsensors were inserted into the cortex and sapwood of the main stem of each tree (Fig. 1, left) at breast height. For minimal-invasive insertion, a piercing needle (precision needle; Precision, Hanover, MD, USA) was inserted into the cortex and sapwood up to the desired depth with the help of a micromanipulator (PreSens GmbH). Afterwards the cannula of the microsensors, which fits exactly into the piercing needle, was inserted and both were locked in position by a clamp of a stand. The needle entry points were sealed with a sealant (Terostat; Henkel) to prevent any diffusion of oxygen from the atmosphere into the stem tissue via the micro-channels formed by the needle. Additionally, an N_2-flush was applied to the entry point to directly check for gas tightness. After the measurement period, the stem was dissected along the insertion channels of the microsensors and the position of the sensors were checked by microscopy (digital microscope Keyence VH-X 600 DSO, Osaka, Japan).

For temperature compensation of oxygen measurements, temperature sensors (Micro-T-type thermocouples with a tip-diameter of 0.7 mm; Driesen & Kern GmbH, Bad Bramstedt, Germany; datalogger Squirell SQ2040; Grant, Cambridge, UK) were attached to the stem surface and inserted into the cortex and sapwood of the main stems (Fig. 1, left). There was no substantial gradient between surface and within-tissue temperatures (data not shown). Measurements of oxygen concentration and temperature were carried out at 5-min intervals. For more details on the measurement principle of the sensors, see Gansert *et al.* (2001), Rolletschek *et al.* (2009), and Wittmann & Pfanz (2015).

The oxygen content in % air saturation was converted into the oxygen concentration (µmol l^{-1}) by the following conversion formula:

$$cO_2[\mu\text{mol l}^{-1}] = \frac{p_{atm} - p_w(T)}{p_N} \times \frac{\%\text{ air saturation}}{100} \times 0.2095 \times \alpha(T) \times 1000\,000 \times \frac{1}{V_M}, \qquad \text{Eqn 4}$$

(p_{atm}, actual atmospheric pressure; p_N, standard pressure (1013 mbar); 0.2095, volume content of oxygen in air; $p_w(T)$, vapor pressure of water at temperature T given in Kelvin; $\alpha(T)$, Bunsen absorption coefficient at temperature T (cm^3(O_2) cm^{-3}); V_M, molar volume (22.414 l mol^{-1})).

Continuous chlorophyll fluorescence measurements. Continuous stem chlorophyll fluorescence was recorded with a 'Monitoring-PAM multi-channel chlorophyll fluorometer' or MONI-PAM (Walz). In this study, we used an arrangement consisting of two oxygen microsensors and two measuring heads (MONI-head/485) (Fig. 1, left), recording PAM fluorescence, temperature and PPFD.

Stems were fixed in MONI-head clips consisting of two aluminium frames (35 × 25 mm). The clip is mounted at a distance of 25 mm from the MONI-head's optical window so that the clip area and longitudinal axis of the MONI-head form an angle of 120°C (Porcar-Castell *et al.*, 2008). The MONI-head-clip includes a laterally mounted 13 × 7 mm area covered by a 1-mm-thick white-reflecting Teflon layer which directs ambient light toward the MONI-head optical window in which the PPFD is measured.

Because our stems covered only a part of the sample holder, we placed black foam behind the samples to exclude possible fluorescence from the background.

In the present study saturating pulses were supplied every 5 min, and yield (or F_v/F_m at night), ETR, PPFD and temperature were recorded for each measuring point. Chlorophyll fluorescence parameters were calculated according to Genty *et al.* (1989). For calculating ETR, the abs values obtained for intact stems with the IPAM (see later) were chosen (for details see Wittmann & Pfanz, 2016).

Data analysis

All statistical data analyses were performed with IBM SPSS Statistics v.25 (IBM Corp., New York, NY, USA). Data were checked for normality using a Shapiro–Wilk test and for homogeneity using Levene's test at $P < 0.05$. Significance of differences between sets of chlorophyll and PPFD-transmittance data was checked by Student's *t*-tests. The tissue effect on chlorophyll-fluorescence data was tested by MANOVA. For pairwise, inter-tissue comparisons, Bonferroni *post-hoc* tests ($P < 0.05$) were applied. Furthermore, for all trees correlations (Spearman rank) of hourly stem cO_2 (µmol l^{-1}) with $R_{d(mod)}$, effective and maximum quantum efficiency of PSII (yield, F_v/F_m), ETR, tissue temperature (T) and PPFD were calculated, as well as

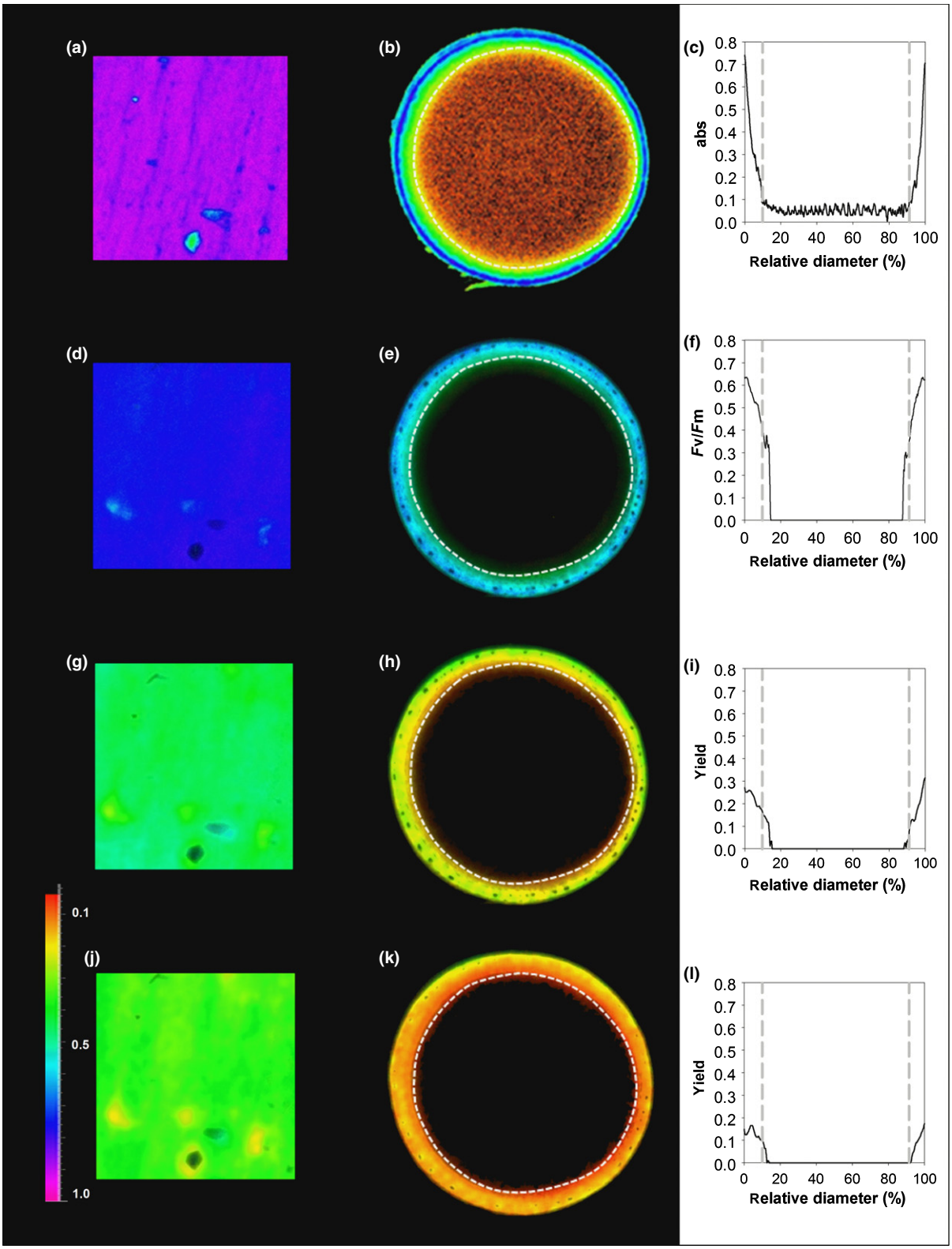

Fig. 2 Imaging the photosynthetically active radiation (PAR)-absorptivity (abs) and photosynthetic quantum efficiency in stems of black poplar. Images of stem surfaces (left; a, d, g, j), and of stem cross-sections (in the middle; b, e, h, k). (a, b) Pattern of PAR-absorptivity (abs), (d, e) of maximum quantum efficiency (F_v/F_m) of photosystem II (PSII), (g, h) of effective quantum efficiency of PSII (yield) at a PAR of 25 µmol photons m^{-2} s^{-1}, (j, k) and of effective quantum efficiency of PSII (yield) at a PAR of 85 µmol photons m^{-2} s^{-1}. (c, f, i, l) Transects taken (from 09:00 h to 15:00 h) from the images of stem cross-sections. Measurements were made on 4-yr-old stems of *Populus nigra* at 20°C. The dashed white and grey lines mark the position of the cambium. PAR-absorptivity and photosynthetic quantum yields are denoted by colour.

cross-correlations with a maximum time lag of ±2 h. For cross-correlations, a positive time lag in hours means that cO_2 lags behind the cross-correlation variable, a negative lag means that the cross-correlation variable lags behind stem cO_2. Two-way ANOVA was used to test for the effects of tissue (cortex vs sapwood), diel period (diurnal vs nocturnal) and their interaction on mean diurnal tissue O_2 (% air sat.), cO_2 (μmol l^{-1}), $R_{d(mod)}$ and fluorescence parameter (yield, F_v/F_m). Therefore, data for all days and trees were pooled. ANOVA tests were done with the General Linear Models (GLM) procedure, after log_{10} transformation if residuals were not normally distributed.

Results

Laboratory experiments

Chlorophyll extraction and tissue absorptivity Highly significant differences between chlorophyll contents and chl*a*/*b* ratios of cortex and wood tissue of 4-yr-old stems of black poplar were found ($P < 0.001$, Table 1).

In Fig. 2, the PPFD-absorptivity (abs) of a stem surface (Fig. 2a) and a stem cross-section (Fig. 2b) are shown. PPFD-absorptivity of the stem surface revealed a largely, homogeneous pattern with a mean value of 0.714 (Fig. 2a; Table 2). However, the abs-image of 4-yr-old stem cross-sections (Fig. 2b,c) showed a steep decrease of PPFD-absorptivity with increasing distance from the stem surface. Behind the cambium PPFD-absorptivity declined immediately to values below 0.1.

Accordingly, mean PPFD-absorptivity of the stem surface was significantly higher than that of the cross-sectioned cortex ($P < 0.001$) and in the same way the mean abs value of the cross-sectioned cortex was significantly higher than that of the cross-sectioned wood tissue ($P < 0.001$, Table 2).

Peridermal PPFD transmission Table 2 shows the PPFD-transmittance of outer bark (= periderm) and total bark (= outer bark plus cortex) as measured on 4-yr-old stems of *Populus nigra* trees. Within the PAR-band (380–720 nm), a mean peridermal PPFD-transmittance of 25% was found, whereas total bark transmitted on average only 2% of the incident PAR.

Light penetration is not stopped at the inner bark level; some light penetrates even the outer plus inner bark to reach the wood fraction within black poplar stems. However, light intensities reaching the wood are very low (Table 2).

Chlorophyll fluorescence pattern of stem surfaces and among stem cross-sections Chlorophyll fluorescence imaging of stem surfaces and cross-sections of stems revealed the highest photochemical activity in the outermost region of stems (Fig. 2d–l). The highest efficiency of PSII was found in the cortex parenchyma near to the stem surface (Fig. 2d,g,j). Transects through the F_v/F_m- and yield-images revealed a sharp decrease of photosynthetic quantum efficiency from the outer cortex to the cambium of the stems (Fig. 2e,h,k). Almost no PSII activity was found in the wood tissue of the stems (Fig. 2; Table 2). Accordingly, mean values of photochemical parameters were significantly lower in the wood as compared to the cortex ($P < 0.001$, Table 2) and highest on surfaces of intact stems (Table 2).

Table 2 Optical and photosynthetic properties of different stem tissues as measured on 4-yr-old stems of *Populus nigra* trees

	Stem tissue		
Parameter	Outer bark	Total bark	
PPFD-transmittance (%) (380–720 nm)	24.93 ± 1.12	2.14 ± 0.22***	
	$Stem_{surface}$	Cortex	Wood
abs	0.817 ± 0.083a	0.446 ± 0.012b	0.095 ± 0.018c
F_v/F_m	0.714 ± 0.059a	0.550 ± 0.073b	0.287 ± 0.096c
Yield (measured at 15 μmol photons m^{-2} s^{-1})	0.607 ± 0.053a	0.319 ± 0.040b	0.154 ± 0.025c
Yield (measured at 25 μmol photons m^{-2} s^{-1})	0.466 ± 0.029a	0.240 ± 0.040b	0.093 ± 0.040c
Yield (measured at 40 μmol photons m^{-2} s^{-1})	0.403 ± 0.026a	0.200 ± 0.036b	0.045 ± 0.048c
Yield (measured at 85 μmol photons m^{-2} s^{-1})	0.358 ± 0.037a	0.150 ± 0.027b	0.000 ± 0.000c

MANOVA	Pillai's trace	*F*	df	Error df
Tissue	< 0.001***	7.75	12	38

Mean ± 1 SD ($n = 10$) for photosynthetic photon flux density (PPFD)-transmittance (%) of outer bark and total bark (= outer bark plus cortex) as well as chlorophyll fluorescence parameter (PPFD-absorptivity (abs), maximum quantum efficiency of phototsystem II (PSII) (F_v/F_m), effective quantum efficiency of PSII (yield)) are given. Chlorophyll fluorescence measurements were performed on surfaces of intact stems and stem cross-sections by means of a standard Imaging-PAM fluorometer (Walz) at 20°C. As area of interest, the cross-sectional area of the corresponding stem tissue (cortex, wood) was chosen. Significant differences between PPFD-transmittance of outer bark and total bark as examined by Student's *t*-tests: ***, $P < 0.001$. MANOVA results regarding tissue effects on parameters are shown (***, $P < 0.001$). Means with the same letter are not significantly different from each other (Bonferroni *post-hoc* test, $P < 0.05$).

Temperature- and oxygen-dependency curves of stem respiration A significant exponential relationship between R_d of cortex and temperature ($r^2 = 0.994$, $P = 0.0029$) and R_d of sapwood and temperature ($r^2 = 0.991$, $P = 0.0044$) was found. The respiratory Q_{10} derived from this relationship was 2.54 for the cortex and 2.31 for the sapwood (Fig. 3a, $P < 0.05$)). Among tissues, R_d of the cortex was significantly higher ($P < 0.05$) as compared to the R_d of the sapwood (Fig. 3a).

The extent to which respiration was inhibited clearly depended on the oxygen availability. Until an oxygen concentration of *c.* 70% air saturation was reached, R_d decreased only slightly. A reduction in oxygen concentration from 100% to 80% air saturation resulted in a reduction of R_d of even 10% (Fig. 3b) in the cortex, whereas in the sapwood R_d was close to a maximum at these concentrations. However, when oxygen concentration decreased below a threshold value (*c.* 70% air sat.), the decline of the oxygen consumption rate got progressively steeper until R_d reached zero; R_d of cortex was reduced to zero at concentrations below 60 µmol l^{-1} (21% air sat.) those of sapwood even below 100 µmol l^{-1} (35% air sat.) (Fig. 3b). The oxygen concentration in the medium necessary for half-maximum respiration rates was 118 µmol l^{-1} (42% air sat.) for cortex and 156 µmol l^{-1} (55% air sat.) for sapwood of black poplar stems (Fig. 3b).

Field experiments

Continuous measurements of tissue oxygen concentration and chlorophyll fluorescence The effective quantum efficiency of PSII (yield) followed the diel pattern of PPFD and temperature. Over the course of sunny days the initial increase and subsequent decrease in PPFD incident on the black poplar stems (Figs 4a, 5a) were mirrored by an initial decrease and subsequent increase in the effective quantum efficiency of PSII (Figs 4b, 5a). During the day, the course of electron transport rate of PSII (ETR) paralleled the PPFD pattern (Figs 4b, 5b). F_v/F_m remained nearly constant during night and showed a mean of 0.54 (Table 3).

Diurnal changes in cortical O_2 (% air-sat.) and cO_2 (µmol l^{-1}) strongly matched with the diurnal pattern of ETR (Fig. 4). Cortical cO_2 showed large daily fluctuations between on average 233 (24 h min) and 399 µmol O_2 l^{-1} (24 h max.) (Fig. 4; Table 3), which is equivalent to mean O_2 levels of between 82% and 107% of air saturation (Fig. 4; Table 3). The maxima of O_2 (% air sat.) and cO_2 (µmol l^{-1}) in the cortex corresponded well with the daytime maxima in PPFD and ETR (Fig. 4c). Overall, effective quantum efficiency of PSII was the most important driver of cortical cO_2 during daytime (r and r_{max} in Table 4). It was responsible for 68–93% of the variation in cortical cO_2, whereas no significant relationship between cortical cO_2 and $R_{d(mod)}$ was found (Table 4; Fig. 5c). During the night-time, in the absence of photosynthesis, cortical cO_2 was most closely related to $R_{d(mod)}$ (Table 4).

On the contrary, no correspondence was apparent in the diurnal course of ETR and the course of O_2 (% air-sat.) and cO_2 (µmol l^{-1}) in the sapwood (Figs 4c, 5b). Among all investigated

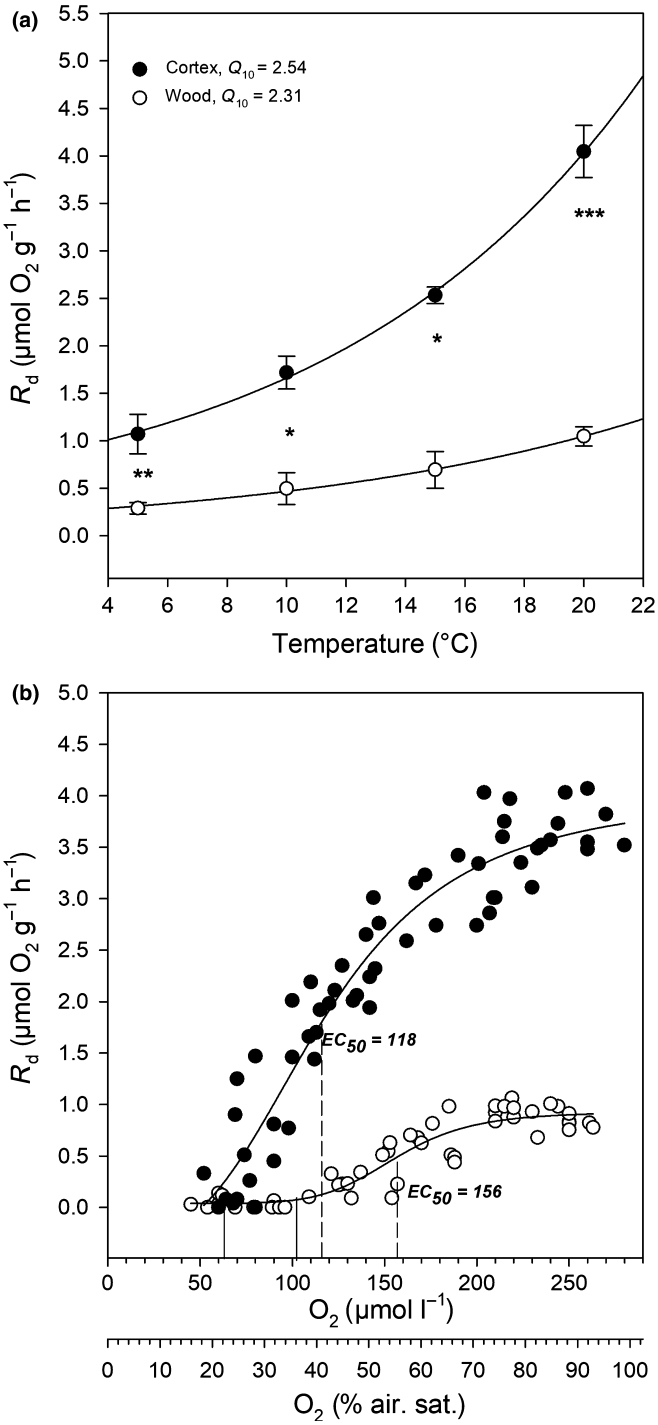

Fig. 3 Temperature- and oxygen-dependency curves of dark respiration in black poplar stems. (a) Mean dark respiration (R_d) (µmol O_2 g^{-1} h^{-1}) of isolated cortex and sapwood tissue in dependence of temperature ($n = 10$); (b) dark respiration (R_d) (mmol O_2 g^{-1} h^{-1}) of isolated cortex and sapwood tissue in dependence of tissue oxygen concentration (µmol l^{-1}) or (% air sat.). Dashed lines mark the dissolved oxygen concentration at which half-maximum respiration rate (EC_{50}) is obtained; solid lines mark the dissolved oxygen concentration below which total inhibition of respiration occurs. Asterisks indicate significant differences between tissues as examined by Student's t-tests (*, $P < 0.05$; **, $P < 0.01$; ***, $P < 0.001$).

time periods, sapwood cO_2 was most closely related to $R_{d(mod)}$ (Table 4; Fig. 5d). Overall, > 80% of the variation in sapwood cO_2 could be explained by $R_{d(mod)}$ (Table 4). Thereby, sapwood cO_2 showed daily fluctuations between on average 258 and 361 µmol O_2 l^{-1} (Table 3). Maximum oxygen concentrations were measured between 07:30 and 09:15 h, at tissue temperatures of 4.1–9.5°C and PAR values between 10 and 18 µmol photons m^{-2} s^{-1}, and thus, did not match with diurnal maxima in PPFD and ETR. Minimum concentrations were observed at *c.* 14:00 h (Fig. 5), when woody tissue temperature maxima of 18.5–25.5°C were reached (Fig. 4a).

Oxygen concentrations in the sapwood were always below atmospheric concentration (100% air saturation corresponds to 21% O_2 concentration in the atmosphere) (Table 4; Fig. 4c), whereas in the cortex under illumination even a net increase in tissue oxygen level of up to 110% of air saturation (superoxia) was apparent (Fig. 4c).

There was a significant effect of diel period on mean diurnal tissue O_2 (% air sat.) (Table 3), but no significant effect of tissue and the interaction (tissue × diel period) was found. By contrast, both effects, tissue and diel period, were significant for $R_{d(mod)}$.

Discussion

Laboratory experiments

Oxygen gas-exchange measurements of isolated stem tissues Among tissues, dark respiration (R_d) of the cortex was significantly higher than that of the sapwood, implying higher respiratory oxygen consumption and thus a potentially higher risk for hypoxia in the cortex as compared to sapwood tissues. In stems, respiring parenchyma cells can be found in the inner bark, vascular cambium and xylem. The proportion of living cells often decreases with depth from the inner bark and cambium (Stockfors & Linder, 1998; Pfanz *et al.*, 2002), which results in differences in the rate of cellular respiration. For *Pseudotsuga menziesii* Franco and ponderosa pine trees Pruyn *et al.* (2002a,b) reported

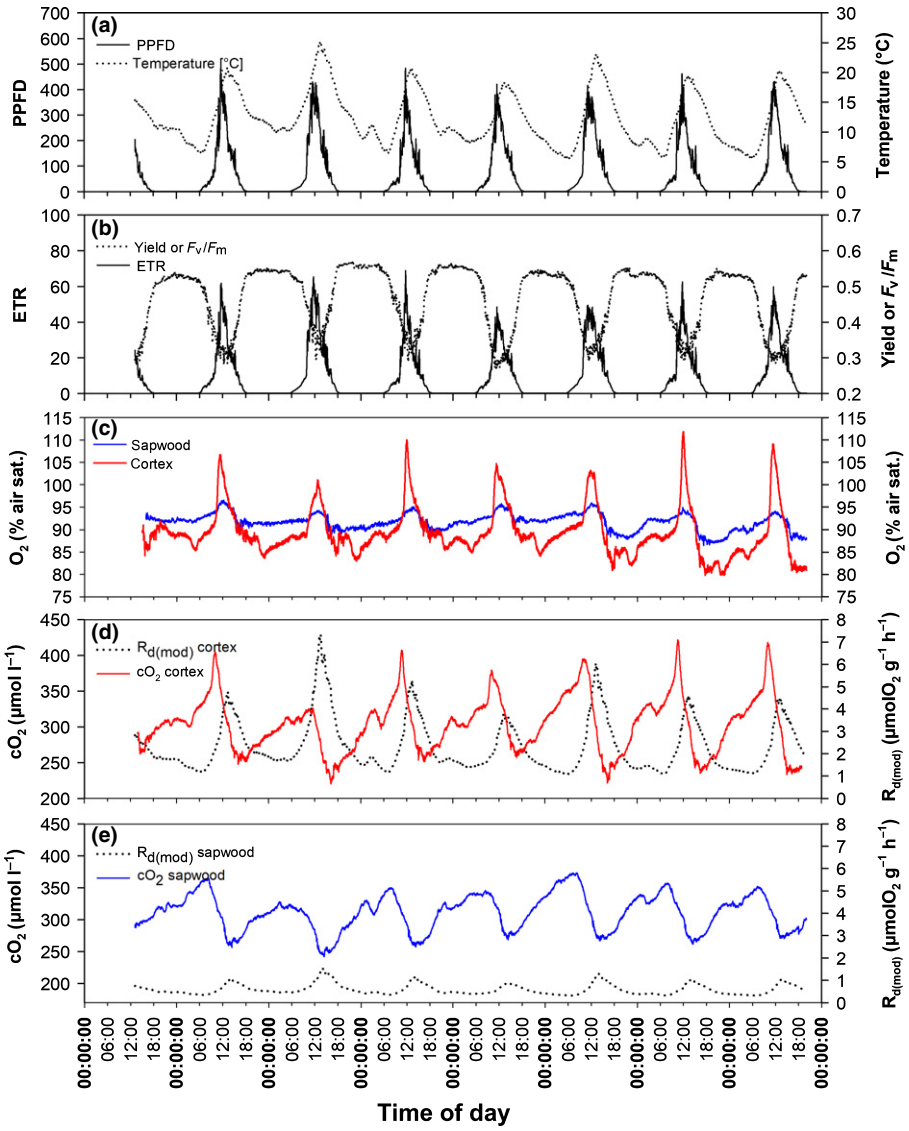

Fig. 4 Mean diurnal courses of (a) photosynthetic proton flux density (PPFD) (µmol photons m^{-2} s^{-1}) at stem surface and stem temperature (°C); (b) quantum efficiency of photosystem II (PSII) (yield or F_v/F_m) and electron transport rate (ETR) (µmol e^- m^{-2} s^{-1}) of black poplar stems; (c) dissolved oxygen concentration in the cortex and sapwood (% air sat.); (d) dissolved oxygen concentration in the cortex (µmol l^{-1}) compared to dark respiration rate of cortex tissue ($R_{d(mod)}$) (µmol O_2 g^{-1} h^{-1}); (e) dissolved oxygen concentration in the sapwood (µmol l^{-1}) compared to dark respiration rate of sapwood tissue ($R_{d(mod)}$) (µmol O_2 g^{-1} h^{-1}). Means of tree 1–3 ($n = 3$) are given.

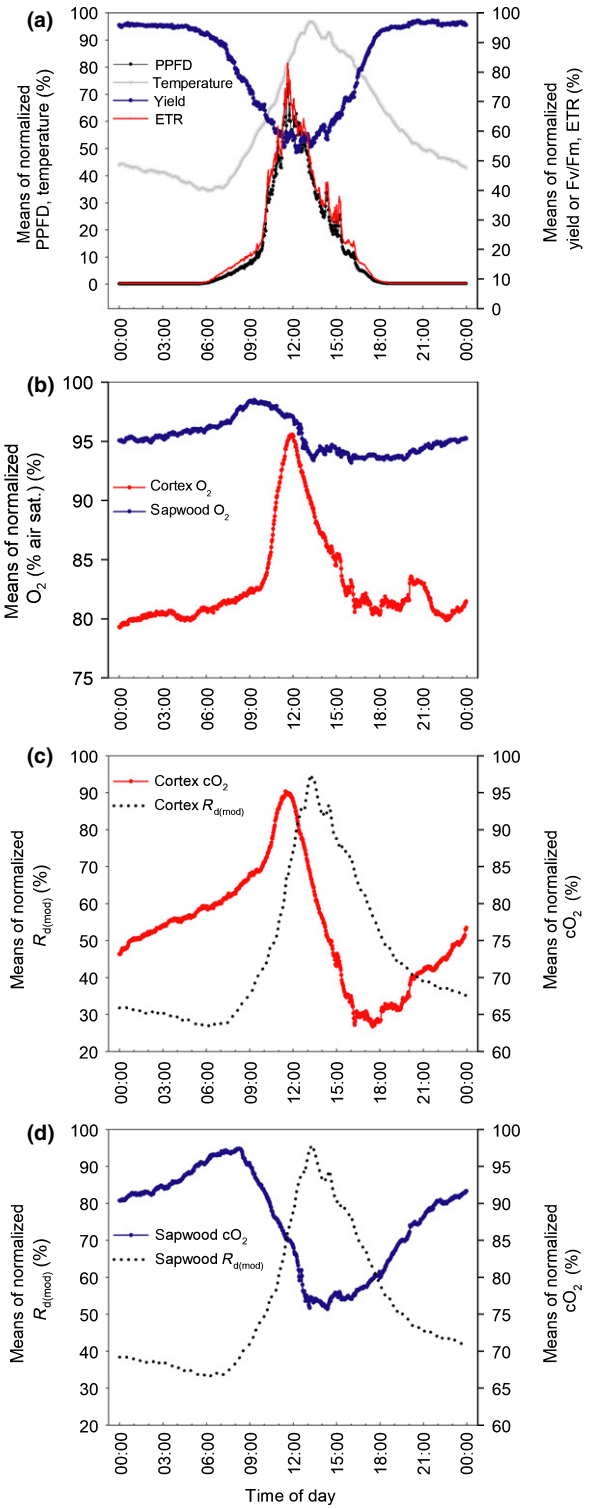

Fig. 5 Normalized diurnal courses of (a) PPFD (μmol photons m^{-2} s^{-1}) at stem surface, stem temperature (°C), quantum efficiency of photosystem II (PSII) (yield or F_v/F_m) and electron transport rate (ETR) (μmol e^- m^{-2} s^{-1}) of black poplar stems; (b) dissolved oxygen concentration in the cortex and sapwood (% air sat.); (c) dissolved oxygen concentration in the cortex (μmol l^{-1}) compared to dark respiration rate ($R_{d(mod)}$) of cortex tissue (μmol O_2 g^{-1} h^{-1}); (d) dissolved oxygen concentration in the sapwood (μmol l^{-1}) compared to dark respiration rate of sapwood tissue ($R_{d(mod)}$) (μmol O_2 g^{-1} h^{-1}). Values are normalized by the respective daily maxima. Means ($n = 21$) are given.

substantially higher rates of R_d for inner bark than for sapwood tissues. Respiration of the inner bark was 2–3 times greater than sapwood respiration in Douglas fir trees, and 50–70% higher in outer compared to inner sapwood (Pruyn *et al.*, 2002b).

Oxygen-depletion curves of isolated stem tissues showed the extent to which respiration is inhibited under hypoxic conditions (Fig. 3b). Overall, the degree of inhibition of R_d depended on the tissue and the tissue cO_2. A reduction in oxygen concentration from 100% to 80% air saturation resulted in a reduction of R_d of 10% (Fig. 3b) in cortex tissues, whereas in the sapwood R_d was close to a maximum at these concentrations. The R_d of isolated cortex tissues was reduced to zero at concentrations below 50 μmol l^{-1}; those of woody tissues already at concentrations below 100 μmol l^{-1} (Fig. 3b); 50 and 100 μmol l^{-1} are (at 20°C, 1013 hPa) equivalent to 3.7% (17.67% air saturation) and 7.4% O_2 (35.33% air sat.), respectively. Spicer & Holbrook (2005) reported that sapwood respiration in *Fraxinus americana* and *Tilia canadensis* was unchanged at oxygen levels above 10% and 5% (v/v). At 1% O_2 – a value lower than actually observed in the sapwood – respiration was reduced by just 65% and 75% for *T. canadensis* and *F. americana*, respectively (Spicer & Holbrook, 2005). We found a more distinct effect of reduced O_2 on stem parenchyma respiration at these extreme oxygen levels (Fig. 3), and a rather moderate effect of reduced O_2 on R_d at O_2 levels typical of stem tissues in spring (see *in situ* measurements below).

Chlorophyll fluorescence pattern of stem surfaces and among stem cross-sections Transects through the F_v/F_m and $\Delta F/F'_m$ images of stem cross-sections revealed that photosystem II (PSII) activity and thus oxygen release was restricted to the stem cortex (Fig. 2). The highest maximum and effective quantum efficiency of PSII was found in the cortex parenchyma near to the stem surface (Fig. 2d,g,j). Almost no PSII activity was found in the sapwood of the stems (Fig. 2; Table 2). These findings are in agreement with the observed photosynthetically active radiation (PAR)-absorptivity (abs) images (Fig. 2) and pigment contents (Table 1). Several studies showed that the number of chloroplasts per cell is highest in the outer fraction (80 μm) of the stem cortex and fairly abruptly decreases with depth, leaving only a few chloroplasts per cell in the phloem and the living cells of the xylem (see Pfanz *et al.*, 2002). This might also explain why chlorophyll fluorescence imaging of stem surfaces and cross-sections of 4-yr-old black poplar stems revealed the highest PSII activity in the outermost region of stems (Fig. 2d–l), which is consistent with previous reports on other tree species (Berveiller *et al.*, 2007; Wittmann & Pfanz, 2016). Measurements of Photosynthetic Photon Flux Density (PPFD) transmittance further revealed that light intensities reaching the wood were not high; on average 2% of PAR was transmitted through outer and inner bark and were available to drive photomorphogenesis and photochemistry of the woody tissues.

Field experiments

Continous measurements of tissue oxygen concentration and chlorophyll fluorescence This study has shown for the first

Table 3 Mean ± 1 SD for diurnal and nocturnal averages and 24 h minimum and maximum of tissue O_2 (% air sat.), O_2 concentration (μmol l^{-1}), modelled tissue dark respiration rates ($R_{d(mod)}$) and fluorescence parameter representing quantum efficiency of phototsystem II (PSII) (yield, F_v/F_m) of black poplar stems

Parameter	Tissue	Diel period				Effect	df	F	P value
		Diurnal avg.	Nocturnal avg.	24 h min.	24 h max.				
O_2 (% air sat.)	Cortex	94.09 ± 3.71	89.81 ± 2.71	82.49 ± 5.70	106.63 ± 7.27	Tissue	1	0.211	0.647
	Sapwood	93.52 ± 2.98	91.09 ± 2.64	87.40 ± 3.64	96.50 ± 2.89	Diel period	1	19.37	**0.000**
						Tissue × diel period	1	1.466	0.231
O_2 (μmol l^{-1})	Cortex	328.96 ± 30.63	301.32 ± 12.80	233.06 ± 25.59	398.82 ± 44.73	Tissue	1	0.272	0.604
	Sapwood	300.98 ± 19.13	323.37 ± 22.13	258.20 ± 27.21	360.51 ± 33.17	Diel period	1	0.214	0.645
						Tissue × diel period	1	19.44	**0.000**
$R_{d(mod)}$ (μmol g^{-1} h^{-1})	Cortex	3.26 ± 0.73	1.64 ± 0.26	1.19 ± 0.03	5.26 ± 1.66	Tissue	1	5.034	**0.000**
	Sapwood	0.82 ± 0.13	0.48 ± 0.06	0.37 ± 0.07	1.11 ± 0.36	Diel period	1	1.102	**0.000**
						Tissue × diel period	1	0.014	0.112
Quantum efficiency of PSII (yield or F_v/F_m)	Stem*	0.391 ± 0.04	0.544 ± 0.04	0.276 ± 0.07	0.569 ± 0.03	Diel period	1	263.3	**0.000**

For calculation, data of all days and trees ($n = 3$) were pooled. In addition, results of two-way ANOVA for the effects of tissue (cortex vs sapwood) and diel period (diurnal vs nocturnal) and their interaction on the parameters are shown. *P*-values for significant effects are shown in bold.
*Measurements were made on stem surfaces.

time *in situ* that hypoxia appears in the cortex and sapwood of *Populus nigra* trees during times of zero sap flow in spring (before leaf flush). The literature had already provided some (indirect) evidence for hypoxic metabolism in the stem of plants. In maize, alcohol dehydrogenase (ADH) transcript accumulates to a higher degree in the stem vasculature than in the epidermis (Nakazono *et al.*, 2003); a common plant response to O_2 limitation. The cortex (phloem) of stems also carries a number of enzymes that belong to a prominent class of hypoxia-induced genes, and may play a role in counteracting anoxic injury (Geigenberger, 2003).

However, until now, oxygen levels or concentrations were measured only in the sapwood of trees. The lowest O_2 concentrations reported for woody tissue were *c.* 14–24% of air sat. (Eklund, 1990; Mancuso & Marras, 2003; Spicer & Holbrook, 2005) and the highest (72–95% of air sat.) were closer to atmospheric levels (Eklund, 1990; Pruyn *et al.*, 2002a; Wittmann & Pfanz, 2015). In general, reported sapwood O_2 concentrations varied with species, tree age, sapwood depths, and mode of sampling and analytic techniques (e.g. Wittmann & Pfanz, 2015), and were often lower than measured O_2 concentrations in the sapwood and cortex of this study.

Diurnal O_2 levels fluctuated strongly in black poplar stems (Figs 4, 5). Over the course of the day oxygen levels in the sapwood were always lower than the atmospheric concentration, indicating hypoxic conditions within the tissue, due to a combination of increased consumption and reduced supply (i.e. no active transpiration stream before bud burst). During the daytime, the O_2 concentration in the sapwood steadily decreased, because respiratory oxygen consumption of the wood parenchyma increased exponentially with temperature. With decreasing temperatures, recovery from hypoxia sets in due to decreased respiratory activity and increased oxygen solubility (Fig. 5d). During day and night $R_{d(mod)}$ was the strongest driving factor for sapwood cO_2 (Table 4). Over 80% of diurnal changes in sapwood cO_2 could be explained by respiration rates. The changes in the explanatory power of this relationship with diel time period (Table 4) might be the result of diurnal changes in the water status and cell turgor pressure of the stem cells (Etzold *et al.*, 2013; Mencuccini *et al.*, 2017; Salomón *et al.*, 2017). A reduced cell water status and turgor pressure during daytime has been suggested as a constraint on stem respiratory metabolism (Saveyn *et al.*, 2007; Steppe *et al.*, 2007, 2015; Mencuccini *et al.*, 2017; Salomón *et al.*, 2017). Accordingly, the $R_{d(mod)}$–cO_2 relationship was strongest in the daytime between 07:00 and 12:00 h (Table 4), at a time when the cortex can be expected to be replete with carbohydrates and turgor pressures are high.

On the contrary, subambient oxygen levels in the cortex steadily increased during daytime illumination, which even led to a diel period of superoxia of up to 110% air sat. (Fig. 4c). During the daytime, corticular cO_2 was driven largely by the effective quantum efficiency of PSII (Table 3), and no relationship between $R_{d(mod)}$ and cO_2 was apparent (Fig. 5c). Yield values measured *in vivo* on black poplar stems (Fig. 4; Table 3) were consistent with previous reports on other trees (Berveiller *et al.*, 2007; Wittmann & Pfanz, 2007, 2008). The observed drop in F_v/F_m values during night (on average 0.6) can be explained by the low night temperatures of up to 5°C, which might induce an active downregulation of F_v/F_m to avoid low-temperature stress. According to Solhaug & Haugen (1998), maximum quantum yield of PSII in the bark of *Populus tremula* was considerably reduced below temperatures of 5°C. Because the reduction in F_v/F_m depended on sun exposure and on phellem thickness, they concluded that photoinhibition was partly responsible. At temperatures below 5°C a significant reduction in F_v/F_m also has

Table 4 Correlation coefficients of mean hourly tissue cO_2 ($\mu mol\ l^{-1}$) and dark respiration (R_d), effective and maximum quantum efficiency of phototsystem II (PSII) (yield, F_v/F_m), electron transport rate (ETR), stem temperature (T) and photosynthetic photon flux density (PPFD) of 4-yr-old stems of *Populus nigra* in March 2014

			R_d		Yield or F_v/F_m		ETR		T		PPFD	
Time period	Tree	Tissue	r	r_{max}	r	r_{max}	r	r_{max}	r	r_{max}	r	r_{max}
Day (07:00–12:00 h)	1	Cortex	0.136	−0.628 (−2)$^+$	−0.684*	=	0.499$^+$	=	0.136	−0.628 (−2)$^+$	0.553$^+$	=
Day (12:00–18:00 h)			0.237	−0.454 (−2)$^+$	−0.927*	=	0.877*	=	0.227	−0.456 (−2)$^+$	0.895*	=
Night (18:00–07:00 h)			−0.732*	=	−0.058	−0.204 (2)	–	–	−0.718*	=	–	–
Day (07:00–12:00 h)	1	Sapwood	−0.986*	=	0.225	−0.647 (2)$^+$	−0.750*	=	−0.986*	=	−0.677*	=
Day (12:00–18:00 h)			−0.701*	−0.806 (−1)*	−0.432$^+$	−0.535 (1)$^+$	0.077	−0.370 (−2)	−0.701*	−0.806 (−1)*	0.163	−0.320 (−2)
Night (18:00–07:00 h)			−0.925*	=	−0.174	−0.591 (2)$^+$	–	–	−0.918*	=	–	–
Day (07:00–12:00 h)	2	Cortex	0.293	−0.438 (−2)$^+$	−0.603*	=	0.547$^+$	=	0.289	−0.445 (−2)$^+$	0.588*	=
Day (12:00–18:00 h)			0.314	−0.454 (−2)$^+$	−0.936*	=	0.802*	=	0.314	−0.454 (−2)$^+$	0.849*	=
Night (18:00–07:00 h)			−0.696*	=	−0.209	−0.293 (2)	–	–	−0.694*	=	–	–
Day (07:00–12:00 h)	2	Sapwood	−0.938*	=	0.297	−0.561 (2)$^+$	−0.700*	=	−0.933*	=	−0.632*	=
Day (12:00–18:00 h)			−0.692*	−0.824 (−1)*	−0.368$^+$	−0.480 (2)$^+$	−0.244	−0.623 (−1)$^+$	−0.692*	−0.824 (−1)*	−0.143	−0.545 (−1)$^+$
Night (18:00–07:00 h)			−0.882*	=	−0.117	−0.277 (2)	–	–	−0.882*	=	–	–
Day (07:00–12:00 h)	3	Cortex	0.168	−0.529 (−2)$^+$	−0.569*	=	0.506*	=	0.168	−0.529 (−2)$^+$	0.553$^+$	=
Day (12:00–18:00 h)			0.201	−0.510 (−2)$^+$	−0.686*	=	0.593*	=	0.265	−0.559 (−2)$^+$	0.504$^+$	=
Night (18:00–07:00 h)			−0.655*	=	−0.333	=	–	–	−0.654*	=	–	–
Day (07:00–12:00 h)	3	Sapwood	−0.983*	=	0.371	−0.550 (1)$^+$	−0.537$^+$	=	−0.977*	=	−0.565$^+$	=
Day (12:00–18:00 h)			−0.859*	=	−0.432$^+$	=	−0.590$^+$	=	−0.855*	=	−0.566$^+$	=
Night (18:00–07:00 h)			−0.865*	=	−0.173$^+$	−0.510 (2)$^+$	–	–	−0.861*	=	–	–

r, Spearman rank correlation coefficient; r_{max}, maximum correlation of time-lagged variables, with time lag in hours given in parenthesis. '=', r_{max} equals r. '–' no data available.
Grey shadows indicate the highest r resp. r_{max} per time-period.
Significance: *, $P < 0.001$; +, $P < 0.01$.

been reported for 1- to 2-yr-old beech and birch stems (Wittmann & Pfanz, 2007).

However, high diurnal temperatures in the cortex and sapwood enhanced the respiratory oxygen consumption and increased the diel oxygen deficit. Accordingly, phases of high O_2 depletion compared to atmospheric concentrations occurred over the course of the day especially at high temperatures (Figs 4, 5), which can be attributed to the significant exponential relationship found between temperature and R_d of cortex and sapwood (Fig. 3). However, the oxygen concentrations measured in the cortex and sapwood of black poplar stems were never reduced below 80% of air saturation (Figs 4, 5). Referring to our laboratory experiments, these *in vivo* concentrations would lead to a rather moderate reduction in respiratory activity of *c.* 10% (Fig. 3).

Implications of corticular photosynthesis in the movement of oxygen within trees

Phases of superoxia found in the daytime could result in a radial efflux of O_2 from the cortex to the atmosphere or could favour axial O_2 diffusion within the cortex. The latter will depend on the degree and distribution of cortical gas-spaces, and the degree and distribution of respiratory demand (Armstrong & Armstrong, 2014). However, subambient O_2 concentrations, found in the early afternoon and night in black poplar stems (Fig. 4), could favour a radial O_2 influx from the atmosphere to the cortex and wood. According to Fick's law of diffusion, the direction of movement depends on the gas concentration difference between sources and sinks as well as the axial and radial gas diffusion gradients within stems. Several authors argued that the xylem (Sorz & Hietz, 2008), cambium (Hook *et al.*, 1972) and bark layers (Lendzian, 2006; Wittmann & Pfanz, 2008, 2015) can be significant barriers to radial gas diffusion. Because diffusion occurs much faster in air than in water, diurnal variation in the ratio of gas to water concentration in the xylem, cambium and cortex also can have an important influence on diffusion rates (Sorz & Hietz, 2006; Teskey *et al.*, 2008).

In the present study, resistances to axial and radial O_2 diffusion were not assessed. Nevertheless, we found no increase in sapwood oxygen levels during phases of cortical superoxia of up to 110% of air sat. (Fig. 4, 5), which hints rather at low radial oxygen diffusion rates from the cortex to the wood or a high local oxygen demand from the cortex itself. In young stems, peridermal conductances of water vapour in the order of $0.010\ \mathrm{mol\ m^{-2}\ s^{-1}}$ have been reported (Wittmann & Pfanz, 2008). Diffusive conductance in the gas phase for water vapour ($\mathrm{mol\ m^{-2}\ s^{-1}}$) can be converted into that for O_2 by dividing it through the ratio of the diffusion coefficients for water vapour and O_2 ($\mathrm{mm^2\ s^{-1}}$) (24.2/20.3 = 1.10; at $T = 20°C$). Taking the concentration gradients of this study (daytime average of 94% air sat., nocturnal average of 90%, 24 h O_2 minimum of 82% (see Table 4)) and the peridermal conductance to O_2 ($\mathrm{mol\ m^{-2}\ s^{-1}}$), we calculated influx rates of oxygen from the atmosphere into the cortex in the order of $0.005\ \mu\mathrm{mol\ m^{-2}\ s^{-1}}$ in the daytime, $0.010\ \mu\mathrm{mol\ m^{-2}\ s^{-1}}$ at night and $0.016\ \mu\mathrm{mol\ m^{-2}\ s^{-1}}$ at the 24 h minimum of tissue O_2 concentration. Thus, inward diffusion from the atmosphere into the stem is rather low. The increase in oxygen concentration can thus be clearly attributed to PS_{cort} and is not the result of inward diffusion of O_2. The O_2 produced by PS_{cort} inside the stem can be consumed by strongly oxygen-demanding regions such as the vasculature or cambium, or oxygen might be internally translocated (e.g. via diffusion in cortical gas-spaces or dilution in the aqueous phase of the cortex cells or xylem sap).

Conclusions

The combination of microsensor quantification and chlorophyll fluorescence imaging of this study added further information about the mechanisms and the physiological significance of corticular photosynthesis (PS_{cort}). Although the fate of oxygen in stems is not completely known, it has huge implications on the energy metabolism of the involved tissues. In actively dividing stems (i.e. before bud burst), the main problems for respiratory energy metabolism are a shortage of oxygen (due to high metabolic rates and diffusive resistances within tissues) and depletion of carbohydrates, which are one of the substrates of R_d. The results of this study show that the oxygen provided by PS_{cort} during daytime illumination can help in maintaining adequate rates of respiration and alleviating the adverse effects of xylem sap depletion before bud burst.

Acknowledgements

The authors wish to thank Christa Kosch from the Laboratory of Applied Botany and Monika Fillippek from the Botanical Garden of the University Duisburg-Essen for their enthusiastic technical and horticultural support.

Author contributions

C.W. conceived the study, performed the research, analysed and interpreted the data and wrote the manuscript; H.P. wrote and proofread the manuscript.

References

Armstrong W, Armstrong J. 2014. Plant internal oxygen transport (diffusion and convection) and measuring and modelling oxygen gradients. In: van Dongen JT, Licausi F, eds. *Low-oxygen stress in plants. Oxygen sensing and adaptive responses to hypoxia.* Berlin, Germany: Springer, 267–297.

Ávila E, Herrera A, Tezara W. 2014. Contribution of stem CO_2 fixation to whole-plant carbon balance in nonsucculent species. *Photosynthetica* **52**: 3–15.

van Bel AJE, Knoblauch M. 2000. Sieve element and companion cell: the story of the comatose patient and the hyperactive nurse. *Australian Journal of Plant Physiology* **27**: 477–487.

Berveiller D, Kierzkowski D, Damesin C. 2007. Interspecific variability of stem photosynthesis among tree species. *Tree Physiology* **27**: 53–61.

Bloemen J, McGuire MA, Aubrey DP, Teskey RO, Steppe K. 2013. Transport of root-respired CO_2 via the transpiration stream affects aboveground carbon assimilation and CO_2 efflux in trees. *New Phytologist* **197**: 555–565.

Cannell MGR, Thornley JHM. 2000. Modelling the components of plant respiration: some guiding principles. *Annals of Botany* **85**: 45–54.

Cernusak LA, Cheesman AW. 2015. The benefits of recycling: how photosynthetic bark can increase drought tolerance. *New Phytologist* **208**: 995–997.

Cernusak LA, Marshall JD. 2000. Photosynthetic refixation in branches of Western White Pine. *Functional Ecology* **14**: 300–311.

van Dongen JT, Licausi F. 2015. Oxygen sensing and signaling. *Annual Review of Plant Biology* **66**: 345–376.

Eklund L. 1990. Endogenous levels of oxygen, carbon dioxide and ethylene in stems of Norway spruce trees during one growing season. *Trees* **4**: 150–154.

Eklund L. 2000. Internal oxygen levels decrease during the growing season and with increasing stem height. *Trees* **14**: 177–180.

Etzold S, Zweifel R, Ruehr NK, Eugster W, Buchmann N. 2013. Long-term stem CO_2 concentration measurements in Norway spruce in relation to biotic and abiotic factors. *New Phytologist* **197**: 1173–1184.

Gansert D, Burgdorf M, Lösch R. 2001. A novel approach to the *in situ* measurement of oxygen concentrations in the sapwood of woody plants. *Plant, Cell & Environment* **24**: 1055–1064.

Geigenberger P. 2003. Response of plant metabolism to little oxygen. *Current Opinion in Plant Biology* **6**: 247–256.

Geigenberger P, Alisdair RF, Gibon Y, Christ M, Stitt M. 2000. Metabolic activity decreases as an adaptive response to low internal oxygen in growing potato tubers. *Biological Chemistry* **381**: 723–740.

Genty B, Briantais JM, Baker NR. 1989. The relationship between the quantum yield of photosynthetic electron transport and quenching of chlorophyll fluorescence. *Biochimica et Biophysica Acta* **990**: 87–92.

del Hierro AM, Kronberger W, Hietz P, Offenthaler I, Richter H. 2002. A new method to determine the oxygen concentration inside the sapwood of trees. *Journal of Experimental Botany* **53**: 559–563.

Hook DD, Brown CL, Wetmore RH. 1972. Aeration in trees. *Botanical Gazette* **133**: 443–454.

Johnsen K, Maier C, Sanchez F, Anderson P, Butnor J, Waring R, Linder S. 2007. Physiological girdling of pine trees via phloem chilling: proof of concept. *Plant, Cell & Environment* **30**: 128–134.

Lammertyn J, Franck C, Verlinden BE, Nicolai BM. 2001. Comparative study of the O_2, CO_2 and temperature effect on respiration between 'Conference' pear cell protoplasts in suspension and intact pears. *Journal of Experimental Botany* **52**: 1769–1777.

Lendzian K. 2006. Survival strategies of plants during secondary growth: barrier properties of phellems and lenticels towards water, oxygen, and carbon dioxide. *Journal of Experimental Botany* **57**: 2535–2546.

Linder S, Troeng E.. 1981. The seasonal variation in stem and coarse root respiration of a 20-year-old Scots pine (*Pinus sylvestris* L.). *Mitteilungen der Forstlichen Bundes-Versuchsanstalt Wien* **142**: 125–139.

Mancuso S, Marras AM. 2003. Different pathways of the oxygen supply in the sapwood of young *Olea europea* trees. *Planta* **216**: 1028–1033.

Mencuccini M, Salmon Y, Mitchell P, Höltta T, Choat B, Meir P, O'Grady A, Tissue D, Zweifel R, Sevanto S *et al.* 2017. An empirical method that separates irreversible stem radial growth from bark water content changes in trees: theory and case studies. *Plant, Cell & Environment* **40**: 290–303.

Millar AH, Bergersen FJ, Day DA. 1994. Oxygen affinity of terminal oxidases in soybean mitochondria. *Plant Physiology and Biochemistry* **32**: 847–852.

Mugnai S, Mancuso S. 2010. Oxygen transport in the sapwood of trees. In: Mugnai S, Shabala S, eds. *Waterlogging, signalling and tolerance in plants.* Berlin, Germany: Springer, 61–75.

Nakazono M, Qiu F, Borsuk LA, Schnable PS. 2003. Laser-capture microdissection, a tool for the global analysis of gene expression in specific plant cell types: identification of genes expressed differentially in epidermal cells or vascular tissues of maize. *Plant Cell* **15**: 583–596.

Pfanz H, Aschan G, Langenfeld-Heyser R, Wittmann C, Loose M. 2002. Ecology and ecophysiology of tree stems: corticular and wood photosynthesis. *Naturwissenschaften* **89**: 147–162.

Porcar-Castell A, Pfündel E, Korhonen E, Juurola E. 2008. A new monitoring PAM fluorometer (MONI-PAM) to study the short- and long-term acclimation of photosystem II in field conditions. *Photosynthesis Research* **96**: 173–179.

Powers EM, Marshall JD. 2011. Pulse labeling of dissolved ^{13}C-carbonate into tree xylem: developing a new method to determine the fate of recently fixed photosynthate. *Rapid Communications in Mass Spectrometry* **25**: 33–40.

Pruyn ML, Gartner BL, Harmon ME. 2002a. Respiratory potential in sapwood of old versus young ponderosa pine trees in the Pacific Northwest. *Tree Physiology* **22**: 105–116.

Pruyn ML, Gartner BL, Harmon ME. 2002b. Within-stem variation of respiration in *Pseudotsuga menziesii* (Douglas-fir) trees. *New Phytologist* **154**: 359–372.

Rolletschek H, Stangelmayer A, Borisjuk L. 2009. Methodology and significance of microsensor-based oxygen mapping in plant seeds – an overview. *Sensors* **9**: 3218–3227.

Saglio PH, Rancillac M, Bruzan F, Pradet A. 1994. Critical oxygen pressure for growth and respiration of excised and intact roots. *Plant Physiology* **76**: 151–154.

Salomón RL, De Schepper V, Valbuena-Carabaña M, Gil L, Steppe K. 2017. Daytime depression in temperature-normalised stem CO_2 efflux in young poplar trees is dominated by low turgor pressure rather than by internal transport of respired CO_2. *New Phytologist* **217**: 586–598.

Saveyn A, Steppe K, Lemeur R. 2007. Daytime depression in tree stem CO_2 efflux rates: is it caused by low stem turgor pressure? *Annals of Botany* **99**: 477–485.

Solhaug KA, Haugen J. 1998. Seasonal variation of photoinhibition of photosynthesis in bark from *Populus tremula* L. *Photosynthetica* **35**: 411–417.

Sorz J, Hietz P. 2006. Gas diffusion through wood: implications for oxygen supply. *Trees* **20**: 34–41.

Sorz J, Hietz P. 2008. Is oxygen involved in beech (*Fagus sylvatica*) red heartwood formation? *Trees* **22**: 175–185.

Spicer R, Holbrook NM. 2005. Within-stem oxygen concentration and sapflow in four temperate tree species: does long-lived xylem parenchyma experience hypoxia? *Plant, Cell & Environment* **28**: 192–201.

Stadler R, Brandner J, Schulz A, Gahrtz M, Sauer N. 1995. Phloem loading by the PmSuc2 sucrose carrier from *Plantago major* occurs into companion cells. *The Plant Cell* **7**: 1545–1554.

Steppe K, Saveyn A, McGuire MA, Lemeur R, Teskey RO. 2007. Resistance to radial CO_2 diffusion contributes to between-tree variation in CO_2 efflux of *Populus deltoides* stems. *Functional Plant Biology* **34**: 785–792.

Steppe K, Streck F, Deslauriers A. 2015. Diel growth dynamics in tree stems: linking anatomy and ecophysiology. *Trends in Plant Science* **20**: 335–343.

Stockfors J, Linder S. 1998. Effects of nitrogen on the seasonal course of growth and maintenance respiration in stems of Norway spruce trees. *Tree Physiology* **18**: 155–166.

Teskey RO, Saveyn A, Steppe K, McGuire MA. 2008. Origin, fate and significance of CO_2 in tree stems. *New Phytologist* **177**: 17–32.

Trumbore SE, Angert A, Kunert N, Muhr J, Chambers JQ. 2013. What's the flux? Unraveling how CO_2 fluxes from trees reflect underlying physiological processes. *New Phytologist* **197**: 353–355.

Vandegehuchte MW, Bloemen J, Vergeynst LL, Steppe K. 2015. Woody tissue photosynthesis in trees: salve on the wounds of drought? *New Phytologist* **208**: 998–1002.

Walker D. 1987. *The use of oxygen electrode and fluorescence probes in simple measurements of photosynthesis.* Sheffield, UK: Sheffield University Press.

Wellburn AR. 1994. The spectral determination of chlorophylls a and b, as well as total carotenoids, using various solvents with spectrophotometers of different resolution. *Journal of Plant Physiology* **144**: 307–313.

Wittmann C, Aschan G, Pfanz H. 2001. Leaf and twig photosynthesis of young beech (*Fagus sylvatica*) and aspen (*Populus tremula*) trees grown under different light intensity regimes. *Basic and Applied Ecology* **2**: 145–154.

Wittmann C, Pfanz H. 2007. Temperature dependency of bark photosynthesis in beech (*Fagus sylvatica* L.) and birch (*Betula pendula* Roth.) trees. *Journal of Experimental Botany* **58**: 4293–4306.

Wittmann C, Pfanz H. 2008. General trait relationships in stems: a study on the performance and interrelationships of several functional and structural parameters involved in corticular photosynthesis. *Physiologia Plantarum* **134**: 636–648.

Wittmann C, Pfanz H. 2015. Bark and woody tissue photosynthesis: a means to avoid hypoxia or anoxia in developing stem tissues. *Functional Plant Biology* **41**: 940–953.

Wittmann C, Pfanz H. 2016. The optical, absorptive and chlorophyll fluorescence properties of young stems of five woody species. *Environmental and Experimental Botany* **121**: 83–93.

Wittmann C, Pfanz H, Loreto F, Centritto M, Pietrini F, Alessio G. 2006. Light-induced reduction of carbon release from branches of birch trees: corticular photosynthesis, photorespiration or inhibition of mitochondrial respiration? *Plant, Cell & Environment* **29**: 1149–1158.